Biochimica et Biophysica Acta 1853 (2015) 481–488

Contents lists available at ScienceDirect

Biochimica et Biophysica Acta

journal homepage: www.elsevier.com/locate/bbamcr

Involvement of aberrant miR-139/Jun feedback loop in human gastric cancer

Yan Zhang [a,1], Wen-Long Shen [a,1], Ming-Lei Shi [a,1], Le-Zhi Zhang [a], Zhang Zhang [a], Ping Li [a], Ling-Yue Xing [a,b], Feng-Yan Luo [a], Qiang Sun [a,*], Xiao-Fei Zheng [c], Xiao Yang [d,**], Zhi-Hu Zhao [a,***]

[a] Institute of Biotechnology, Beijing 100071, China
[b] School of Life Science, Anhui University, Hefei 230601, China
[c] Beijing Institute of Radiation Medicine, 27 Taiping Road, Haidian District, Beijing 100850, China
[d] State Key Laboratory of Proteomics, Genetic Laboratory of Development and Disease, Institute of Biotechnology, Beijing 100071, China

ARTICLE INFO

Article history:
Received 1 June 2014
Received in revised form 28 November 2014
Accepted 2 December 2014
Available online 10 December 2014

Keywords:
MiR-139
Jun
Gastric cancer
Feedback loop

ABSTRACT

Accumulating evidence indicates that some miRNAs could form feedback loops with their targets to fine-tune tissue homeostasis, while disruption of these loops constitutes an essential step towards human tumorigenesis. In this study, we report the identification of a novel negative feedback loop formed between miR-139 and its oncogenic target Jun. In this loop, miR-139 could inhibit Jun expression by targeting a conserved site on its 3′-UTR, whereas Jun could induce miR-139 expression in a dose dependent manner through a distant upstream regulatory element. Interestingly, aberration in this loop was found in human gastric cancer, where miR-139 was down-regulated and inversely correlated with Jun expression. Further functional analysis showed that restored expression of miR-139 in gastric cancer cells significantly induces apoptosis, and inhibits cell migration and proliferation as well as tumour growth through targeting Jun. Thus, our data strongly suggests a role of aberrant miR-139/Jun negative feedback loop in the development of human gastric cancer and miR-139 as a potential therapeutic target for gastric cancer. Given that miR-139 and Jun are deregulated in many cancers, our findings here might have broader implication in other types of human cancers.

1. Introduction

MicroRNAs (miRNAs) are a class of ~22 nucleotides that are single strand non-coding RNAs that typically repress target genes at post-transcriptional level. A large number of studies have implicated miRNAs in almost all kinds of human cancers, and altered miRNA levels can result in aberrant expression of gene products that may contribute to cancer development [1–3].

Recent studies have found that miRNAs often form composite feedback or feedforward loops with their targets, which contributes to robustness of biological processes [4], decreases noise in gene regulation systems [5], and might provide a mechanism of high information flow for the coordinate and adaptable control of miRNA and transcription factor target regulons [6]. These feedback loops might function in normal development as well as in inflammatory response and cancer [7–13].

In this study, we analysed the functional enrichment of miR-139 putative targets, suggesting that miR-139 might play important roles in cancer-related functions and Jun might play central roles in miR-139-mediated functions, and then showed that miR-139, down-regulated in human gastric cancer, might play tumour suppressive roles through regulating the expression of Jun, an important component of the activator protein-1 (AP-1) transcription factor. Conversely, we also observed that Jun could induce miR-139 expression, probably through a distant upstream regulatory region. Hence, we provide the first evidence that Jun is regulated by miR-139 and the Jun/miR-139 feedback loop might be involved in human gastric cancer.

2. Materials and methods

2.1. Plasmids

AP1-luc luciferase reporter construct was made by inserting AP1 responsive element fused to a minimal TA promoter into multiple cloning sites in pGL3-basic reporter construct (Promega, Madison, USA). For the expression of miR-139, genomic fragment of human miR-139 precursor was amplified by PCR and subcloned into pIRES2-EGFP (Clontech).

* Correspondence to: Q. Sun, Institute of Biotechnology, 20 Dongdajie, Beijing 100071, China. Tel.: +86 10 66948821(O).
** Correspondence to: X. Yang, Institute of Biotechnology, 20 Dongdajie, Beijing 100071, China. Tel./fax: +86 10 63895937(O).
*** Correspondence to: Z.-H. Zhao, Institute of Biotechnology, 20 Dongdajie, Fengtai District, Beijing 100071, China. Tel.: +86 10 66948775(O).
E-mail addresses: Sunqiang1975@126.com (Q. Sun), yangx@bmi.ac.cn (X. Yang), zhaozh@bmi.ac.cn (Z.-H. Zhao).
[1] The authors wish it to be known that, in their opinion, the first three authors should be regarded as joint first authors.

http://dx.doi.org/10.1016/j.bbamcr.2014.12.002
0167-4889/

The C-Jun 3′-UTR was cloned into the pGL3-CM as previously described between the *Bgl* II and *Mlu* I sites [3]. Overlapping PCR was performed to mutate the miR-139 target site in the Smad4 3′-UTR, using two additional primers, and the products were subcloned into pGL3-CM.

R (WT)-luc was constructed by cloning the distal region upstream of miR-139 into pGL3-promoter reporter construct, and R(ΔJunBS)-luc was obtained by mutating Jun binding site through overlapping PCR.

2.2. Cell culture and transfection

AGS (gastric carcinoma, ATCC CRL-1739), SGC-7901 (gastric carcinoma) and SNU-16 (gastric carcinoma, ATCC CRL-5974) were cultured in Roswell Park Memorial Institute formulation 1640 (RPMI-1640) supplemented with 10% fetal bovine serum. For transient transfections, the cells were transfected with the aforementioned constructs in 6-cm flasks, protein lysates and total RNAs were collected at the indicated time points. For stable transfection, SGC-7901 cells were transfected with the miRNA expression construct or corresponding control construct in 6-well plates and selected using G418.

2.3. Proliferation assay

SGC-7901, AGS and SNU-16 cells transfected as indicated were subject to MTT assay (Life technology) according to the manufacturer's recommendations. Experiments were repeated three times, and data represented as the mean of quadruplicate wells ± SEM.

2.4. Migration and invasion assays

Cells cotransfected with miR-139 and miR-139 inhibitors or corresponding controls were cultured to confluence and then wounded using a white pipette tip. Three wounds were made for each sample, and migration distance was photographed and measured at zero time, after 48 h and 60 h.

For cell invasion assay, cells were seeded on matrigel-coated polycarbonate membrane insert in a transwell apparatus and maintained in RPMI-1640. RPMI-1640 containing 10% FBS was added to the lower chamber. After incubation for 12 h at 37 °C, cells on the top surface of the insert were removed and cells that migrated to the bottom surface of the insert were fixed and stained by crystal violet and then subjected to microscopic inspection.

2.5. Flow cytometry

For the quantification of apoptosis, the cells were washed in cold PBS, incubated with Annexin V-PE and 7-Amino-Actinomycin D (7-AAD) (Southern Biotech, Birmingham, AL, USA) for 15 min in the dark and analysed within 1 h. Flow cytometry was performed using a Fluorescence-Activated Cell Sorting (FACS) Calibur Flow Cytometer with CellQuest 3.0 software (BD Biosciences, San Jose, CA, USA) or winMDI software (V2.9; Purdue University, West Lafayette, USA). For the measurement of cell cycle, 2–3 × 10^6 cells were fixed in 70% cold ethanol, treated with RNase A and stained with propidium iodide (Sigma). All analyses were performed in triplicate, and 20,000 gated events/samples were counted.

2.6. Soft agar assays

Transfected cells were plated in 0.25% agar on top of 0.5% agar, both containing 10% FBS in RPMI-1640. After two weeks, colonies with 50 cells or more were counted.

2.7. Local tumour growth

Tumour cell suspensions (10^7 cells/100 μl PBS) of either overexpression or mock cell lines were inoculated into the thigh of female nude mice. 40 days after implantation, mice were killed and tumours were weighted and photographed.

2.8. Luciferase reporter assay

Luciferase reporter assays were performed as described [3]. Briefly, the reporter plasmids were co-transfected using lipofectamine 2000 reagent (Life technology) with the miR-139 expression plasmid or miR-139 antisense oligos and the vector phRG-TK (Promega), which expresses synthetic Renilla luciferase to normalize the transfection efficiency. Luciferase activities were measured using the Dual-Luciferase Reporter Assay reagent (Promega) on a LB 960 Centro XS3 luminometer (Berthold Technologies, GmbH & Co. KG, Bad Wildbad, Germany). Each experiment was performed in triplicate, and the data represent the mean ± SD of three independent experiments.

2.9. Real-time RT-PCR for miRNA and mRNA analysis

Total RNA was isolated with Trizol reagent (Life technology), and Reverse transcription was performed using with oligo dT primers and random N6 primers for mRNA and stem-loop RT primer for miRNA with Superior III RT supermix (Innogene biotech, Beijing, China). The real-time PCR primers used are available on request. Real-time PCR was performed using the IQ5 system (BioRad) with UltraSYBR Mixture (Innogene), and expression was quantified relative to a housekeeping gene GAPDH for mRNA and U6 for miRNA. All experiments were repeated at least three times.

2.10. Western blot

Western blots were carried out using antibodies against Jun (#9165, Cell Signalling Technology, Danvers, MA, USA), p21 (#2946, Cell Signalling Technology, Danvers, MA, USA), c-Myc (#9402, Cell Signalling Technology, Danvers, MA, USA), Cyclin D1 (#2978, Cell Signalling Technology, Danvers, MA, USA) β-Actin (A5316, Sigma) and GAPDH (CW0101, Cowin Biotech, Beijing, China).

2.11. ChIP-qPCR

ChIP was performed using EZ-Magna ChIP™ G-Chromatin immunoprecipitation Kit (Millipore, 17-409, Darmstadt, Germany) following manufacturer's guide with Jun antibody (Cell Signalling Technology, #9165) or IgG control (#2729, Cell Signalling Technology). ChIPed DNA was subjected to qPCR analyses using regulatory region primers (F: TCGGTGTCAGCATCACACAA; R: GGAGTGTGGGTGAGTCACTG) and miR-139 locus primers (F: CAGACTCCGGCTTCAGTTGT; R: AGGAGGCA GGAGCTGGAATA).

Fig. 1. MiR-139 directly inhibits Jun expression. A, cross predicted miR-139 targets were subjected for KEGG pathways analysis, and the target-pathway network was visualized in Cytoscape. B, bars show betweenness centrality of the top 10 targets. C, bars show relative miR-139 expression as assessed by RT-qPCR in SGC-7901 cells transfected with miR-139 constructs or inhibitors as indicated; western blots show that Jun protein levels were inhibited by miR-139 and reversed by miR-139 inhibitors. D, top: PAR-CLIP data compiled by Starbase were visualized in UCSC browser. Ago CLIPed putative miR-139 binding site was marked red. Bottom: sequence alignment of putative miR-139-binding site in the Jun-3′-UTR. Lines show Watson–Crick pairing. Unpaired region in mutated constructs were shown in grey and underlined. E, AP-1 responsive reporter activity was inhibited by miR-139 and reversed by miR-139 inhibitors, pGL3-basic as negative reporter control. F, overexpression of miR-139 reduced the luciferase activity of the wild-type Jun-3′-UTR reporter (Luc-Jun (WT)), compared to negative vector control (pGL3-CM), whereas this regulation was abolished when the miR-139 target-binding site in Jun-3′-UTR was mutated (Luc-Jun (Δ)) as indicated.

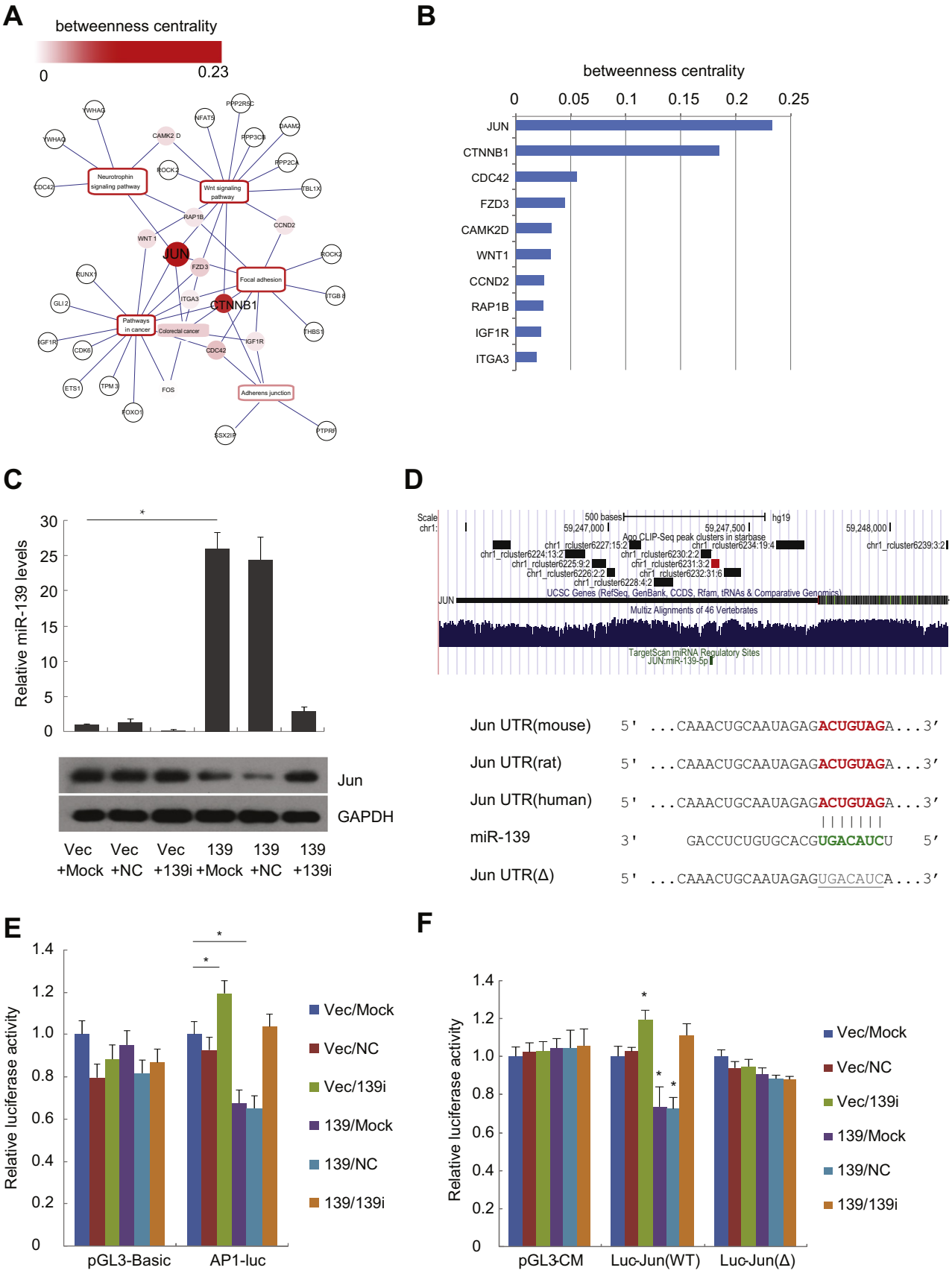
A
betweenness centrality
0
0.23
YWHAG
PPP2R5C
NFATC
CAMK2 D
DAAM2
YWHAQ
PPP3CB
PPP2CA
ROCK2
CDC42
Neurotrophin signaling pathway
Wnt signaling pathway
TBL1X
RAP1B
CCND2
WNT 1
JUN
ROCK2
FZD 3
RUNX1
Focal adhesion
ITGB 8
GLI 2
ITGA3
CTNNB1
Pathways in cancer
Colorectal cancer
THBS1
IGF1R
IGF1R
CDK6
CDC42
ETS1
TPM 3
FOS
Adherens junction
FOXO1
ESX2IP
PTPRF
B
betweenness centrality
0
0.05
0.1
0.15
0.2
0.25
JUN
CTNNB1
CDC42
FZD3
CAMK2D
WNT1
CCND2
RAP1B
IGF1R
ITGA3
C
Relative miR-139 levels
30
25
20
15
10
5
0
*
Jun
GAPDH
Vec +Mock
Vec +NC
Vec +139i
139 +Mock
139 +NC
139 +139i
D
Scale
chr1:
500 bases
hg19
59,247,000
59,247,500
59,248,000
Ago CLIP-Seq peak clusters in starbase
chr1_rcluster6227:15:2
chr1_rcluster6234:19:4
chr1_rcluster6239:3:2
chr1_rcluster6224:13:2
chr1_rcluster6230:2:2
chr1_rcluster6225:9:2
chr1_rcluster6231:3:2
chr1_rcluster6226:2:2
chr1_rcluster6232:31:6
chr1_rcluster6228:4:2
UCSC Genes (RefSeq, GenBank, CCDS, Rfam, tRNAs & Comparative Genomics)
JUN
Multiz Alignments of 46 Vertebrates
TargetScan miRNA Regulatory Sites
JUN:miR-139-5p
Jun UTR(mouse) 5' ...CAAACUGCAAUAGAGACUGUAGA...3'
Jun UTR(rat) 5' ...CAAACUGCAAUAGAGACUGUAGA...3'
Jun UTR(human) 5' ...CAAACUGCAAUAGAGACUGUAGA...3'
miR-139 3' GACCUCUGUGCACGUGACAUCU 5'
Jun UTR(Δ) 5' ...CAAACUGCAAUAGAGUGACAUCA...3'
E
Relative luciferase activity
1.4
1.2
1.0
0.8
0.6
0.4
0.2
0
*
*
pGL3-Basic
AP1-luc
Vec/Mock
Vec/NC
Vec/139i
139/Mock
139/NC
139/139i
F
Relative luciferase activity
1.4
1.2
1.0
0.8
0.6
0.4
0.2
0
*
*
*
pGL3-CM
Luc-Jun(WT)
Luc-Jun(Δ)
Vec/Mock
Vec/NC
Vec/139i
139/Mock
139/NC
139/139i

2.12. Chromosome conformation capture (3C) assay

To determine chromatin interaction frequency between miR-139 upstream regulatory element and miR-139 locus, 3C assay was preformed largely as described [14]. Briefly, SGC-7901 cells were cross-linked by 1% formaldehyde. After cross-linking, nuclei were isolated and digested with *Pst* I restriction enzyme (NEB). The digested nuclei were diluted and intra-complex ligated with T4 DNA ligase (NEB), after reverse cross-linking by proteinase K (Thermo Scientific), ligation frequencies of restriction fragments are analysed by PCR, using primers specific for the restriction fragments of interest (available upon request), all 3C-PCR products were validated by sanger sequencing.

2.13. Bioinformatic analysis

MiR-139 expression profiling data in gastric cancer were downloaded from NCBI GEO database, comparison between gastric cancer and normal tissues were done by Wilcoxon test, and data were plotted with beanplot R package.

TargetScan6.2 (http://www.targetscan.org), PicTar(http://pictar.mdc-berlin.de), PITA (genie.weizmann.ac.il/pubs/mir07/mir07_prediction.html) and Starbase (http://starbase.sysu.edu.cn) were used to predict miR-139 targets. MiR-139 targets were predicted and downloaded from the respective databases with default or stringent settings and then compared and combined with these databases. Only

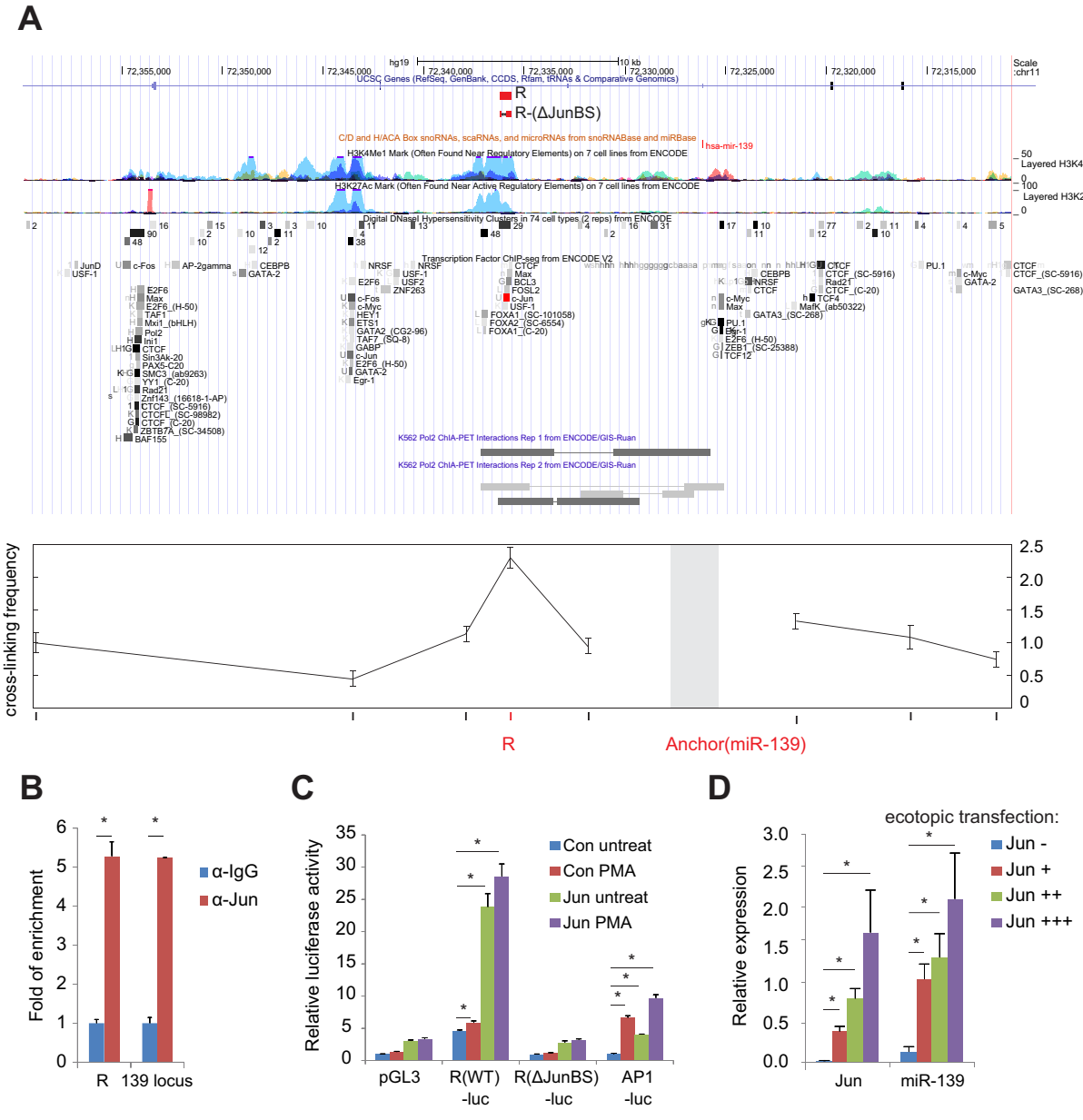

Fig. 2. Jun positively regulates miR-139 expression. A, top: genomic context of miR-139 locus. ENCODE data was obtained from UCSC website (http://genome.ucsc.edu/); there is an H3K3Me and K3K27Ac peak approximately 10 Kb upstream of miR-139 (locus), wherein clustered ChIP-seq data indicates Jun binds to. RNA polymerase II ChIA-PET data from K562 cells indicates that this region might loop to miR-139 locus. Sub-cloned fragments (R) and correspondent mutants (R-ΔJunBS) for reporter assay were marked red. Bottom: The cross-linking frequency of miR-139 (anchor) with the 8 sites as indicated around miR-139 genome context was determined and plotted. B, binding of Jun on regulatory region (R) and miR-139 (locus) were confirmed by ChIP-qPCR. C, regulatory element (R (WT)-luc) conferred increased luciferase activity and Jun responsiveness compared to negative vector control (pGL3), whereas these effects were largely impaired when the Jun binding site was deleted (R(ΔJunBS)-luc). D, gradient ectopic transfection of Jun increased miR-139 levels dose-dependently.

targets that cross proved by at least 2 methods were selected for further analyses. Gene ontology analysis and pathway enrichment analysis were done in DAVID website (http://david.abcc.ncifcrf.gov). The target-pathway network was analysed and visualized in cytoscape software.

2.14. Statistical analysis

Student t tests were performed to assess the significance of treatments vs. controls. Significance of differences in miR-139 levels between normal and gastric cancer tissues was tested by Wilcoxon rank sum test. The relationship between the expression of miR-139 and Jun in gastric cells and tissues was determined using the Spearman rank correlation. $P < 0.05$ was considered statistically significant.

3. Result

3.1. MiR-139 negatively regulates Jun expression

Down-regulation of miR-139 has been reported in several kinds of human cancers [15,16], and therefore a tumour suppressive role was proposed for miR-139, however, its exact role and the underlying mechanisms remain elusive. Computational predictions, based on Starbase data from PAR-CLIP experiments [17] combined with pre-compiled miRNA target databases identified an array of genes as putative targets of miR-139. Pathway analysis on these candidate targets indicated cancer-related pathways as top pathways that miR-139 might regulate (Supplementary Fig. S1A), and gene ontology analysis indicated that miR-139 targets might play important roles in transcription regulation, cell proliferation and migration (Supplementary Fig. S1B). Interestingly, one of the candidate target Jun, a member of activator protein 1 (AP-1) family, was found to be in the centre of target-pathway (Figs. 1A and 1B) and target-function networks (Supplementary Fig. S2). Importantly, all of the methods we used predicted Jun as a miR-139 putative target.

We therefore examined whether miR-139 could repress Jun expression. Indeed, protein levels of Jun were reduced upon miR-139 overexpression in SGC-7901, AGS and SNU-16 cells, which could be readily reversed by miR-139 inhibitors (Fig. 1C and Supplementary Figs. S5A and S5B). Inhibition of miR-139 induced c-Jun and its target c-Myc expression (Supplementary Figs. S5C and S5D). Meanwhile, miR-139 inhibited Jun-mediated AP-1 activity, as assessed by AP-1 responsive reporter assay (Fig. 1E). We were also able to observe that expression of Jun canonical targets c-Myc, Baculoviral IAP Repeat-Containing 5 (BIRC5, Survivin) and Cyclin D1, were significantly down-regulated upon miR-139 overexpression, which could be rescued by Jun restoration (Supplementary Fig. S5E–S5G). Furthermore, computational analysis revealed that Jun 3′-UTR harbours one putative binding site for miR-139 which is conserved across various species, and this target site was also identified in a high throughput Ago PAR-CLIP study [18] (Fig. 1D). To confirm the potential interaction experimentally, a reporter construct was made by sub-cloning human Jun 3′-UTR downstream of the firefly luciferase coding sequence, and cotransfected into SGC-7901 cells with miR-139-expressing construct and/or miR-139 inhibitors. Overexpression of miR-139 decreased luciferase activity as compared to negative controls, while miR-139 inhibitors increased luciferase activity and reversed miR-139-mediated repression; furthermore, mutation

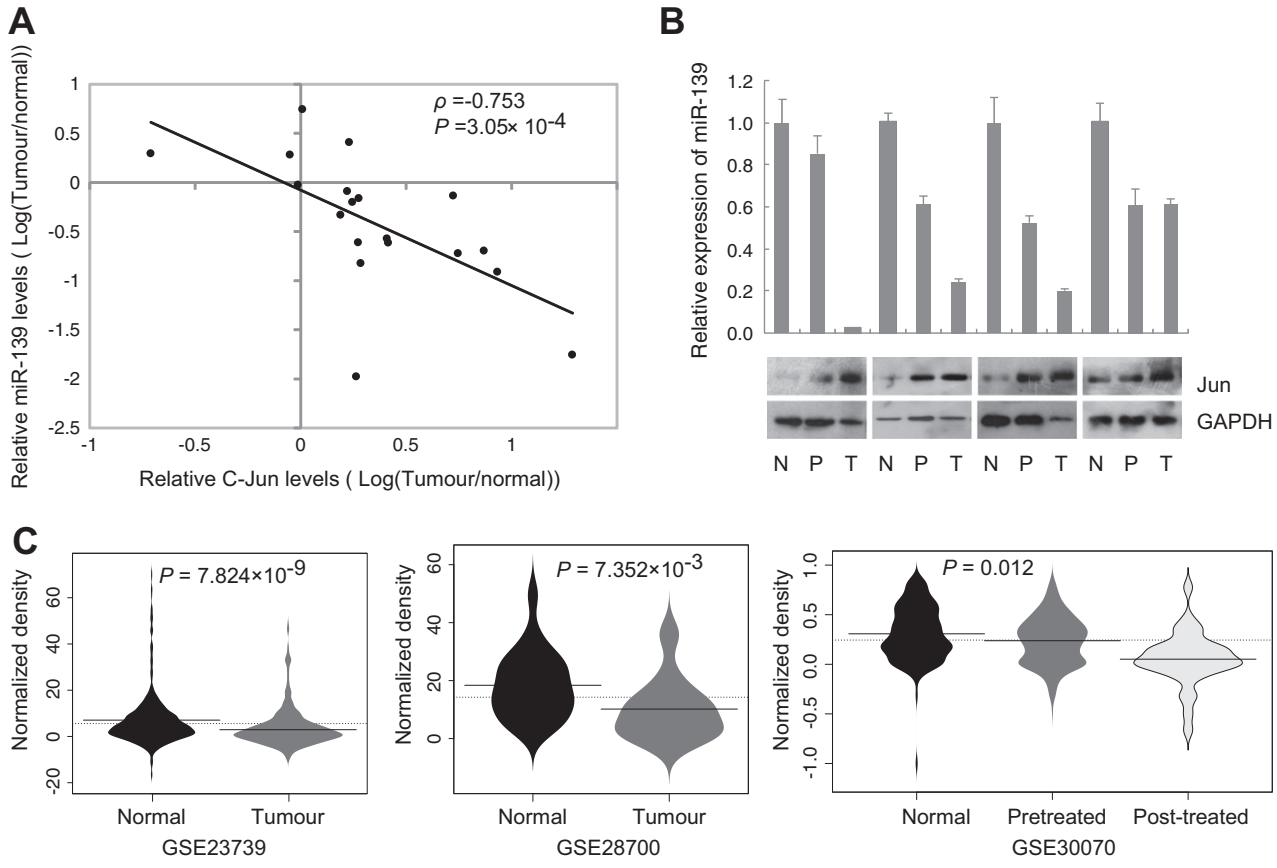

Fig. 3. Inverse correlation between miR-139 and Jun in gastric cancer tissues. A, miR-139 and Jun expression in gastric cancer tissues were normalized to normal tissues, showing miR-139 expression was down-regulated in gastric cancer tissues and inversely correlates with Jun. Correlation test was performed by Spearman rank correlation analysis (n = 19). B, representative results of expression profiling of miR-139 (bars, as assessed by RT-qPCR) and Jun (Western blots) in gastric cancer tissues. N refers to normal tissue; P refers to peritumour tissue and T refers to tumour tissue. C, bean plots depicting the distribution of miR-139 levels in normal and gastric cancer (Tumour) tissues or healthy volunteers and gastric cancer patients treated with cisplatin/fluorouracil or not. *P* value indicates significance returned by Wilcoxon rank sum test. Expression profiling data were obtained from GEO datasets.

of the putative miR-139 binding site abolished the effects of miR-139 and miR-139 inhibitors on luciferase activity (Fig. 1F). These findings suggested that miR-139 could regulate Jun expression through a conserved binding site on its 3′-UTR.

3.2. Jun positively regulates miR-139 transcription

In an attempt to explore the mechanisms underlining miR-139's regulation, we explored data from ENCyclopedia Of DNA Elements (ENCODE) project and found a putative regulatory element characterized by H3K4Me1 and H3K27Ac peaks located approximately 10 kb upstream of miR-139 locus, which harboured an AP-1 motif and also captured by Jun ChIP-seq inferred from ENCODE data (Fig. 2A). Jun was confirmed to bind to the potential regulatory element by using ChIP-qPCR assay in both SGC-7901 and SNU-16 cells, strikingly Jun can also bind to miR-139 locus, around which there is no AP-1 motif (Fig. 2B and Supplementary Fig. S3A). Public Chromatin Interaction Analysis by Paired-End Tag Sequencing (ChIA-PET) data indicated that this regulatory element loops to miR-139 locus. To confirm this physical chromatin interaction in gastric cancer cells, we preformed chromosomal conformation capture (3C) assay in SGC-7901 cells. Data shown in Fig. 2A suggests high frequency of cross-link between these two fragments, providing structure basis for Jun binding to miR-139 locus. Further, to validate the enhancer activity of this element, we subcloned it into pGL3 reporter construct, then co-transfected with Jun overexpression plasmid and/or treated with Phorbol-12-myristate-13-acetate (PMA), which induces both Jun level and activity. Reporter assay indicated that the regulatory element (R) conferred approximately 5 times luciferase activity compared to pGL3 negative control, and Jun could dramatically increase activity of this element, whereas when the Jun binding site was deleted (R(ΔJunBS)), the activity as well as Jun responsiveness to PMA was largely impaired (Fig. 2C). Consistently, the gradually increasing Jun expression by ectopic transfection increased miR-139 expression in a dose dependent manner in two tested gastric cancer cells (Fig. 2D and Supplementary Fig. S3B). These data indicate that Jun could induce miR-139, probably through upstream regulatory element, which in turn targets Jun for inhibition, thus forming a negative feedback loop.

3.3. Aberrant miR-139/Jun feedback loop in human gastric cancer

To establish a clinical implication for the miR-139/Jun feedback loop, we checked the expression of miR-139 and Jun in a set of pair-matched gastric cancer samples; as a result, Jun was up-regulated in 16 of 19 cancerous specimens examined. Importantly, increased Jun expression was significantly correlated with decreased miR-139 (Figs. 3A and 3B) (Spearman's $P = -0.753$, $P = 3.05 \times 10-4$), suggesting an involvement of miR-139/Jun feedback loop in human gastric cancer. Downregulation of miR-139 in gastric cancer tissue was also supported by previous microarray datasets and reports [19] (Fig. 3C). We also determined levels of miR-139 and Jun in gastric cancer cell line SGC-7901, AGS and SNU-16, and again found an inverse correlation between expressions of these two genes (Supplementary Fig. S4).

To explore the roles of miR-139/Jun feedback loop in human gastric cancer cells, we carried out experiments in SGC-7901, AGS and SNU-16 cells. We observed that while apoptosis was significantly higher

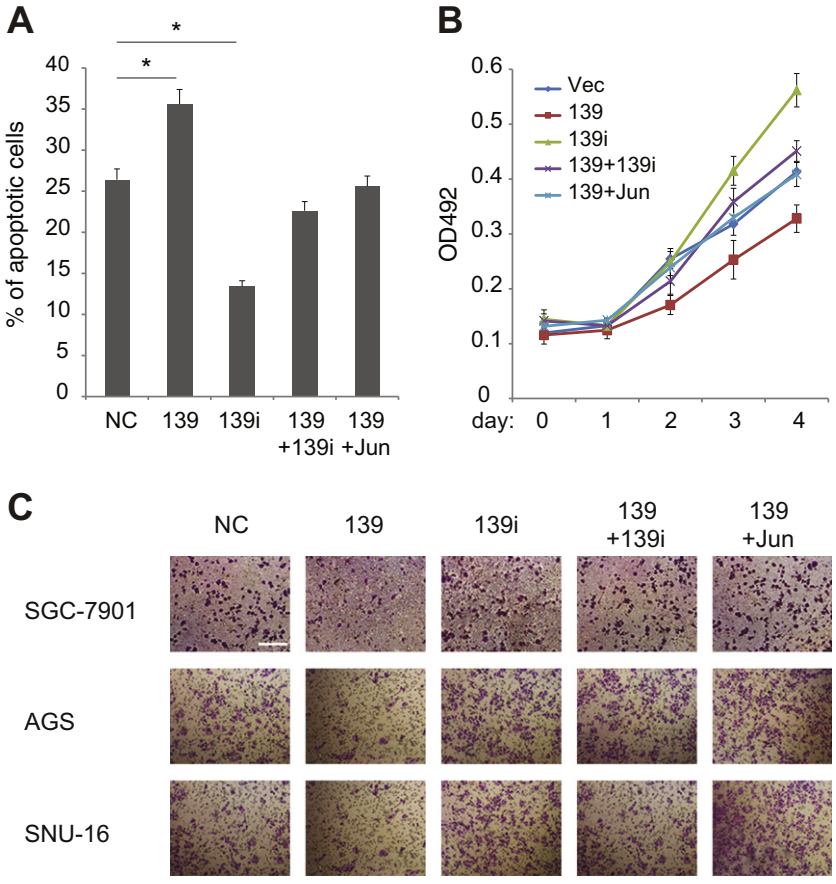

Fig. 4. Involvement of miR-139/Jun feedback loop in gastric cancer cells. A, stable overexpression of miR-139 induced apoptosis, which was reversed by miR-139 inhibitors and rescued by Jun, as assessed by FCM analysis of Annexin V-positive cells. B, growth curve as assayed by MTT assay indicated miR-139 overexpression confers inhibited cell growth in SGC-7901 cells, which was reversed by miR-139 inhibitors and Jun restoration. C, Jun restoration reversed miR-139 inhibition on cell invasion, as assessed by matrigel-coated transwell assay. Scale bar: 200 μm.

(Fig. 4A, Supplementary Fig. S6), cell proliferation, migration and invasion ability were significantly impaired in miR-139 restored cells (Figs. 4B, 4C and Supplementary Fig. S7), which could be reversed by miR-139 inhibitors, supporting a tumour suppressive role of miR-139 in gastric cancer. Importantly, miR-139 likely executes these functions largely by targeting Jun oncogene, as restored Jun expression abolished both the tumour suppressive effects and molecular changes caused by miR-139 overexpression (Fig. 4, Supplementary Fig. S5E–5G and Fig. S6). Next, soft agar assay was performed to test role of miR-139 in colony formation. Overexpression of miR-139 could reduce anchorage independent cell growth, while restoration of Jun could rescue this effect (Fig. 5A). The tumour suppressive role of miR-139 was confirmed in xenograft tumour model, where overexpression of miR-139 resulted in significant smaller tumour growth (Figs. 5B and 5C), which is coincident with increased levels of p21 (WAF/CIP1) and decreased levels of Jun and c-Myc (Fig. 5D). Interestingly, the expression changes of miR-139 and Jun in xenograft tumour model are not as dramatic as in cell line, we reasoned that cells with high level of miR-139 and hence low level of Jun would lose competitive advantage in heterogeneous tumour mixture during the process of tumorigenesis, which is consistent with the fact that miR-139 was frequently reduced, and thus Jun expression increased, in clinical gastric cancer samples.

4. Discussion

MiR-139 is consistently reported to be downregulated in several kinds of tumours, and involved in invasion and metastasis of colorectal cancer and hepatocellular carcinoma by targeting Rho-Kinase 2 [16] and the type I IGF-IR [20] respectively. Here, we preformed functional enrichment analysis on putative miR-139 targets and suggested that miR-139 most likely plays roles in cancer related functions, and oncogenic Jun might play central roles in these complicated miR-139-function networks. Experimental data confirmed that miR-139 inhibits Jun expression and affects gastric cancer via targeting Jun. So it's proposed here that miR-139 exerts tumour suppressive roles by coordinately targeting an array of related oncogenes including Jun.

Previous studies have established that Jun plays essential roles in cell growth, survival, migration and invasion, exerting oncogenic roles in various cancers [21–24]. Activity of Jun is also critical for the initiation and progression of gastric cancer [25,26]. Chemical compounds and biological factors, such as *Helicobacter pylori* [27,28], often act in gastric cancer through regulating Jun, while its regulation by miRNAs in this disease has not been reported yet. Here we showed that miR-139, a miRNA down-regulated in human gastric cancer, could target Jun for expression inhibition, providing a novel level of regulation for Jun in gastric cancer.

Interestingly, we found that Jun could also induce miR-139 expression, probably through an upstream distant regulatory element, which co-localize spatially to miR-139 locus, in a dose dependent manner in gastric cancer cells. Thus, all these data are consistent with the notion that Jun forms a self-limiting feedback loop with miR-139, in which Jun induces miR-139 expression through a distal upstream regulatory element, while miR-139 represses Jun expression to ensure tight control of its oncogenic activity. This unilateral feedback loop is supposed to contribute to homeostasis between oncogenic Jun and tumour suppressive miR-139. Interestingly, despite the high level of Jun in gastric cancer cells, miR-139 stays in low expression level, given that miR-139 is often epigenetic or post-transcriptional inactivated [15,29], we speculate that negative regulatory mechanisms other than Jun induction may dominate the regulation of miR-139 in gastric cancer, which makes the cancer cells insensitive to the lost-controlled Jun expression. In addition to gastric cancer, deregulation of miR-139 and/or Jun was also reported in several kinds of human cancer besides gastric cancer [16,30–32], we therefore could expect a more general role of aberrant miR-139/Jun feedback loop in human tumorigenesis.

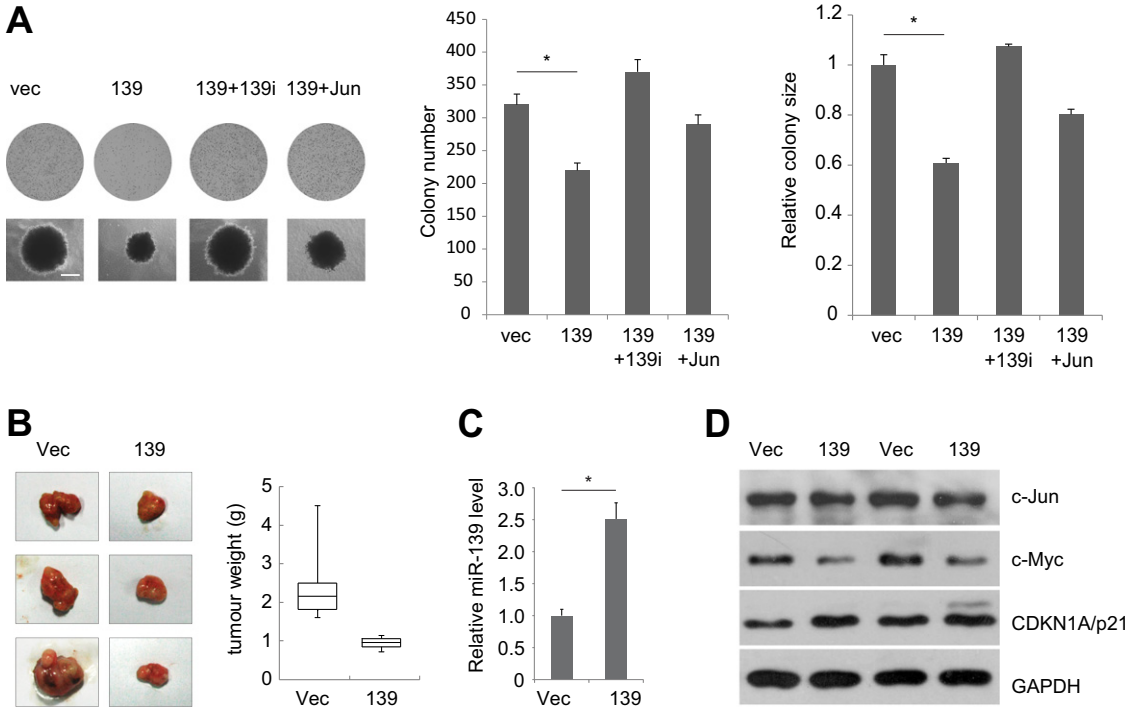

Fig. 5. MiR-139 inhibits tumorigenesis in vitro and in vivo. A, Cells transfected as indicated were grown in soft agar. Representative images were shown. Scale bar: 100 μm. Both colony size and number were reduced by miR-139 overexpression, whereas Jun rescued miR-139 effects on colony growth. B, Xenograft tumours in nude mice over 4 weeks following injection of mice with control cells (Vec) and cells over-expressing miR-139 (139). Total tumour volume difference between the Vec and 139 injected after 4 weeks of growth was statistically significant, as checked by Wilcoxon rank sum test. C, Overexpression of miR-139 was confirmed in xenograft tumours. D, miR-139 inhibited Jun, c-Myc and induced p21 expression in xenograft tumours.

In summary, our study expanded insights into the roles and regulation of miR-139 in gastric cancer, provided the first evidence for direct Jun-miRNA feedback loop in human cancers, which might contribute to our understanding of the complicated mechanisms underlying gastric cancer, and may enhance the development of new therapeutic regimens in treating this disease.

Funding

This work was supported in part by grants from National Basic Research Program of China (NBRPC), National Natural Science Foundation of China (NSFC) and National Key Technology R & D Program of China (NKTRDPC). The grant numbers are as follows: #2013CB966802 (NBRPC), #81372218 (NSFC), #31030026 (NSFC), #31071119 (NSFC), #2012BAI01B07 (NKTRDPC), #2012CB945103 (NBRPC), #2015CB553704 (NBRPC), #81472588 (NSFC) and #30871364 (NSFC).

Acknowledgements

The authors thank Jing Huang and Feng-Lei Li for their assistance with molecular cloning.

Appendix A. Supplementary data

Supplementary data to this article can be found online at http://dx.doi.org/10.1016/j.bbamcr.2014.12.002.

References

[1] Y. Shimono, M. Zabala, R.W. Cho, N. Lobo, P. Dalerba, D. Qian, M. Diehn, H. Liu, S.P. Panula, E. Chiao, Downregulation of miRNA-200c links breast cancer stem cells with normal stem cells, Cell 138 (2009) 592–603.
[2] M. Mori, R. Triboulet, M. Mohseni, K. Schlegelmilch, K. Shrestha, Fernando D. Camargo, Richard.I. Gregory, Hippo signaling regulates microprocessor and links cell-density-dependent miRNA biogenesis to cancer, Cell 156 (2014) 893–906.
[3] Y. Zhang, K.-J. Fan, Q. Sun, A.-Z. Chen, W.-L. Shen, Z.-H. Zhao, X.-F. Zheng, X. Yang, Functional screening for miRNAs targeting Smad4 identified miR-199a as a negative regulator of TGF-β signalling pathway, Nucleic Acids Res. 40 (2012) 9286–9297.
[4] M.S. Ebert, P.A. Sharp, Roles for microRNAs in conferring robustness to biological processes, Cell 149 (2012) 515–524.
[5] M. Voliotis, C.G. Bowsher, The magnitude and colour of noise in genetic negative feedback systems, Nucleic Acids Res. 40 (2012) 7084–7095.
[6] N.J. Martinez, M.C. Ow, M.I. Barrasa, M. Hammell, R. Sequerra, L. Doucette-Stamm, F.P. Roth, V.R. Ambros, A C. elegans genome-scale microRNA network contains composite feedback motifs with high flux capacity, Genes Dev. 22 (2008) 2535–2549.
[7] J. Tsang, J. Zhu, A. van Oudenaarden, MicroRNA-mediated feedback and feedforward loops are recurrent network motifs in mammals, Mol. Cell 26 (2007) 753–767.
[8] O. Ben-Ami, N. Pencovich, J. Lotem, D. Levanon, Y. Groner, A regulatory interplay between miR-27a and Runx1 during megakaryopoiesis, Proc. Natl. Acad. Sci. 106 (1) (2008) 238–243.
[9] F. Petrocca, R. Visone, M.R. Onelli, M.H. Shah, M.S. Nicoloso, I. de Martino, D. Iliopoulos, E. Pilozzi, C.G. Liu, M. Negrini, L. Cavazzini, S. Volinia, H. Alder, L.P. Ruco, G. Baldassarre, C.M. Croce, A. Vecchione, E2F1-regulated microRNAs impair TGFbeta-dependent cell-cycle arrest and apoptosis in gastric cancer, Cancer Cell 13 (2008) 272–286.
[10] D. Iliopoulos, H.A. Hirsch, K. Struhl, An epigenetic switch involving NF-κB, Lin28, Let-7 MicroRNA, and IL6 links inflammation to cell transformation, Cell 139 (2009) 693–706.
[11] H. Zhao, A. Kalota, S. Jin, A.M. Gewirtz, The c-myb proto-oncogene and microRNA-15a comprise an active autoregulatory feedback loop in human hematopoietic cells, Blood 113 (3) (2009) 505–516.
[12] J. Krol, I. Loedige, W. Filipowicz, The widespread regulation of microRNA biogenesis, function and decay, Nat. Rev. Genet. 11 (9) (2010) 597–610.
[13] M. Hatziapostolou, C. Polytarchou, E. Aggelidou, A. Drakaki, George A. Poultsides, Savina A. Jaeger, H. Ogata, M. Karin, K. Struhl, M. Hadzopoulou-Cladaras, D. Iliopoulos, An HNF4α-miRNA inflammatory feedback circuit regulates hepatocellular oncogenesis, Cell 147 (2011) 1233–1247.
[14] J. Dekker, K. Rippe, M. Dekker, N. Kleckner, Capturing chromosome conformation, Science 295 (5558) (2002) 1306–1311.
[15] W. Bao, H.J. Fu, Q.S. Xie, L. Wang, R. Zhang, Z.Y. Guo, J. Zhao, Y.L. Meng, X.L. Ren, T. Wang, Q. Li, B.Q. Jin, L.B. Yao, R.A. Wang, D.M. Fan, S.Y. Chen, L.T. Jia, A.G. Yang, HER2 interacts with CD44 to up-regulate CXCR4 via epigenetic silencing of microRNA-139 in gastric cancer cells, Gastroenterology 141 (2011) 2076–2087 e6.
[16] C.C. Wong, C.M. Wong, E.K. Tung, S.L. Au, J.M. Lee, R.T. Poon, K. Man, I.O. Ng, The microRNA miR-139 suppresses metastasis and progression of hepatocellular carcinoma by down-regulating Rho-kinase 2, Gastroenterology 140 (2011) 322–331.
[17] J.H. Li, S. Liu, H. Zhou, L.H. Qu, J.H. Yang, StarBase v2.0: decoding miRNA-ceRNA, miRNA-ncRNA and protein-RNA interaction networks from large-scale CLIP-Seq data, Nucleic Acids Res. 42 (2014) D92–97.
[18] M. Hafner, M. Landthaler, L. Burger, M. Khorshid, J. Hausser, P. Berninger, A. Rothballer, M. Ascano Jr., A.C. Jungkamp, M. Munschauer, A. Ulrich, G.S. Wardle, S. Dewell, M. Zavolan, T. Tuschl, Transcriptome-wide identification of RNA-binding protein and microRNA target sites by PAR-CLIP, Cell 141 (2010) 129–141.
[19] J. Guo, Y. Miao, B. Xiao, R. Huan, Z. Jiang, D. Meng, Y. Wang, et al., Differential expression of microRNA species in human gastric cancer versus non-tumorous tissues, J Gastroenterol Hepatol. 24 (2009) 652–657.
[20] K. Shen, Q. Liang, K. Xu, D. Cui, L. Jiang, P. Yin, Y. Lu, Q. Li, J. Liu, MiR-139 inhibits invasion and metastasis of colorectal cancer by targeting the type I insulin-like growth factor receptor, Biochem Pharmacol. 84 (2012) 320–330.
[21] R. Eferl, R. Ricci, L. Kenner, R. Zenz, J.-P. David, M. Rath, E.F. Wagner, Liver tumor development: c-Jun antagonizes the proapoptotic activity of p53, Cell 112 (2003) 181–192.
[22] X. Jiao, S. Katiyar, N.E. Willmarth, M. Liu, X. Ma, N. Flomenberg, M.P. Lisanti, R.G. Pestell, c-Jun induces mammary epithelial cellular invasion and breast cancer stem cell expansion, J. Biol. Chem. 285 (2010) 8218–8226.
[23] S. Katiyar, X. Jiao, E. Wagner, M.P. Lisanti, R.G. Pestel, Somatic excision demonstrates that c-Jun induces cellular migration and invasion through induction of stem cell factor, Mol. Cell. Biol. 27 (2007) 1356–1369.
[24] Z. Li, Y. Zhu, M. Yu, D. Ji, Z. Yang, C. Kong, c-Jun is involved in interstitial cystitis antiproliferative factor (APF)-induced growth inhibition of human bladder cancer T24 cells, Urol. Oncol. 31 (2013) 228–233.
[25] W. Shibata, S. Maeda, Y. Hikiba, A. Yanai, K. Sakamoto, H. Nakagawa, K. Ogura, M. Karin, M. Omata, c-Jun NH2-terminal kinase 1 is a critical regulator for the development of gastric cancer in mice, Cancer Res. 68 (2008) 5031–5039.
[26] S.E. Lee, J.W. Lim, H. Kim, Activator protein-1 mediates docosahexaenoic acid-induced apoptosis of human gastric cancer cells, Ann. N. Y. Acad. Sci. 1171 (2009) 163–169.
[27] T. Meyer-ter-Vehn, A. Covacci, M. Kist, H.L. Pahl, Helicobacter pylori activates mitogen-activated protein kinase cascades and induces expression of the proto-oncogenes c-fos and c-Jun, J. Biol. Chem. 275 (2000) 16064–16072.
[28] S. Backert, M. Naumann, What a disorder: proinflammatory signaling pathways induced by Helicobacter pylori, Trends Microbiol. 18 (2010) 479–486.
[29] K. Shen, R. Mao, L. Ma, Y. Li, Y. Qiu, D. Cui, V. Le, P. Yin, L. Ni, J. Liu, Post-transcriptional regulation of the tumor suppressor miR-139-5p and a network of miR-139-5p-mediated mRNA interactions in colorectal cancer, FEBS J. 281 (16) (2014) 3609–3624.
[30] J. Peveling-Oberhag, G. Crisman, A. Schmidt, C. Doring, M. Lucioni, L. Arcaini, S. Rattotti, S. Hartmann, A. Piiper, W.P. Hofmann, M. Paulli, R. Kuppers, S. Zeuzem, M.L. Hansmann, Dysregulation of global microRNA expression in splenic marginal zone lymphoma and influence of chronic hepatitis C virus infection, Leukemia 26 (2012) 1654–1662.
[31] N. Presneau, M. Eskandarpour, T. Shemais, S. Henderson, D. Halai, R. Tirabosco, A.M. Flanagan, MicroRNA profiling of peripheral nerve sheath tumours identifies miR-29c as a tumour suppressor gene involved in tumour progression, Br. J. Cancer 108 (2013) 964–972.
[32] M. Yang, R. Liu, J. Sheng, J. Liao, Y. Wang, E. Pan, W. Guo, Y. Pu, L. Yin, Differential expression profiles of microRNAs as potential biomarkers for the early diagnosis of esophageal squamous cell carcinoma, Oncol Rep. 29 (2013) 169–176.